ROMANIAN JOURNAL OF INFORMATION SCIENCE AND TECHNOLOGY
Volume **28**, Number 1, 2025, 89–102

Higher-Order Model-Free Control Tuned by Fictitious Reference Iterative Tuning for 3D Cranes

Raul-Cristian ROMAN[1], Radu-Emil PRECUP[1, 2, *], and Emil M. PETRIU[3]

[1]Department of Automation and Applied Informatics, Politehnica University of Timisoara, Bd. V. Parvan 2, 300223 Timisoara, Romania

[2]Center for Fundamental and Advanced Technical Research, Romanian Academy – Timisoara Branch, Bd. Mihai Viteazu 24, 300223 Timisoara, Romania

[3]School of Electrical Engineering and Computer Science, University of Ottawa, 800 King Edward, Ottawa, ON, K1N 6N5 Canada

E-mails: raul-cristian.roman@upt.ro, radu.precup@aut.upt.ro*, petriu@uottawa.ca

* Corresponding author

Abstract. The current paper proposes to mix two data-driven algorithms, i.e. Model-Free Control (MFC) and Fictitious Reference Iterative Tuning (FRIT). The MFC algorithm has the main advantage of not using the precise process model, and the FRIT algorithm has the main benefit of determining the optimal parameters of the controller using a set of initial input/output data. Therefore, the mix between these two algorithms improves the performance of the overall control loop with MFC algorithm from one iteration to the next since the optimal parameters of the MFC will be tuned via FRIT. The benefit of this mix is that the parameters of the MFC algorithm are optimally computed using FRIT. An empirical sensitivity study is performed, where higher-order MFC algorithms are tuned via FRIT. The study aims to determine how a higher-order MFC improves the performance of the control loop. The resulting MFC-FRIT algorithms are experimentally validated on the 3D crane laboratory equipment.

Key-words: 3D cranes; fictitious reference iterative tuning; model-free control.

1. Introduction

Data-driven algorithms [1] represent a transformative force in the automatic control domain, combining real-time adaptability with precision tuning to improve the control system loop. By

using real-time data, these algorithms enable control systems to adapt swiftly to changing conditions, thereby enhancing precision and operational efficiency. For instance, for different types of applications, data-driven approaches facilitate automatic process control without the need for complex system models. Therefore, the competitive edge of data-driven automatic control solutions makes them attractive for organizations striving for innovation and operational excellence in today's rapidly evolving industrial landscape.

An important algorithm in the data-driven category is Model-Free Control (MFC) initially proposed by Fliess and Join [2], [3], also organized as intelligent controllers. MFC is widely recognized for its utility since it eliminates the need for an explicit system model and enables swift implementation across diverse applications. The MFC algorithm ensures robust performance despite uncertainties and disturbances by dynamically estimating into a term that gathers both unknown system dynamics and external disturbances. This estimation is made online during the experiment and enables the controller to adjust its control input permanently by effectively compensating for modeling inaccuracies and changes in real-time conditions. Since it was initially proposed and developed, the MFC algorithm has been improved and applied in many impressive and cutting-edge processes including the Quanser AERO [3], cybersecurity processes, where MFC manages to defend against load-altering and Denial of Service attacks [4], in medicine domain, where MFC is implemented in closed-loop neurostimulation for treating epileptiform seizures [5], autonomous vehicles, where MFC and speed-adaptive MFC are used in vehicle navigation [6], cloud and high-performance computing, where MFC is used to administrate the resource harvesting in a computing grid [7], coupled mechatronic systems, where MFC, time-delay estimation MFC, backstepping-based MFC controls 2-DOF and 3-DOF robotic manipulators [8], shape memory alloys processes, where MFC is implemented to control a shape memory alloy spring-based actuator initially [9] and later in [10], forced pendulum, where MFC is based on Kalman Filter and applied to position control [11], tail-sitter unmanned aerial vehicle process, where MFC is applied in hovering mode trajectory tracking control [12], magnetically supported plate [13], tower crane systems, where MFC mixed with the Fictitious Reference Iterative Tuning (FRIT) is used to control the cart, arm angular and the payload position [14]–[16], twin rotor aerodynamic systems, where MFC mixed with fuzzy logic blocks is applied to pitch position control [17], prosthetic hand, where MFC controls the thumb, index, middle, ring and pinky finger [18], 3D cranes, where MFC, sliding mode MFC and fuzzy MFC are applied to payload position control [19].

Another data-driven algorithm, FRIT [20], excels in refining control strategies through iterative adjustments of the controller parameters, delivering enhanced performance. However, its complexity may necessitate specialized expertise for optimal deployment. Like MFC, since FRIT was initially developed and proposed, it has been enhanced and implemented in various processes, including cart systems, where FRIT was used to control the cart position [21], systems with time-delay [22], a switched reluctance generator, a ball screw positioning, two-mass resonance, and a switched reluctance motor stems [23], a benchmark problem with and without time delay, a flexible transmission model by tuning the parameters of a fractional- and integer-order Proportional-Integral-Derivative (PID) controller [24], artificial muscles, where FRIT is mixed with model predictive control [25], asymmetric BoucWen systems, where FRIT improved via pseudo-linearization [26], hexacopter, where FRIT is used to control the roll, pitch and yaw angles [27], and anesthesia processes, where FRIT is used to control hydraulic systems and involves an offline database that stores historical data of the process [28].

In the authors' view, other of the most effective data-driven control algorithms include Active

Disturbance Rejection Control [29]–[31], Model-Free Adaptive Control [32], Iterative Feedback Tuning [33], and Virtual Reference Feedback Tuning [34].

The current paper proposes to blend the MFC and FRIT algorithms since they have complementary features. The MFC algorithm relies on choosing the parameters, this drawback can be solved via FRIT since FRIT iteratively optimally computes the controller parameters after solving a gradient problem via a trust region algorithm, which belongs to the trust region methods described in [35] and [36], which implements a classical search optimization algorithm. The resulting MFC-FRIT algorithm will reduce the tuning effort since the MFC parameters will be optimally tuned, will reduce the deployment time since the timing will be reduced due to automatic tuning, and the overall control loop will be more robust in different conditions, i.e. unexpected disturbances. A disadvantage is that the practitioner will need an initial closed-loop experiment to collect the input/output (I/O) data since FRIT is an iterative algorithm.

Another contribution in the current paper is that an empirical sensitivity study of higher-order MFC algorithms tuned via FRIT is performed. The study aims to determine how a higher-order MFC improves the performance of the control loop.

A higher-order MFC algorithm should precisely approximate the system behavior due to system dynamics. The current paper continues the authors' work of mixing FRIT with other data-driven algorithms to improve the overall control system performance. Initially, the mix between discrete-time first-order MFC denoted as intelligent PID (iPID) with FRIT optimized via the African Vultures Optimization Algorithm (AVOA) was proposed in [16], the mix between continuous-time first-order MFC denoted as intelligent PI (iPI) with FRIT optimized via Slime Mould Algorithm was proposed in [14] and the mix between discrete-time second-order MFC denoted as intelligent P (iP) with FRIT optimized via AVOA was proposed in [15]. All these algorithm mixes, i.e. FRIT-iPID, MFC iPI-FRIT and iP-FRIT, were validated using experiments in the tower crane laboratory setup [37]. The proposed MFC-FRIT algorithms in this paper are experimentally validated on the 3D crane laboratory equipment.

The rest of the paper is structured as follows: in Section 2, the MFC-FRIT algorithm is presented; in Section 3, the 3D crane laboratory equipment is introduced; in Section 4, the experiments with associated empirical sensitivity studies are presented; finally, in Section 5, the conclusions are outlined.

2. The MFC-FRIT Algorithms

2.1. The MFC algorithms

The MFC algorithms are designed around an ultra-local model that is used to replace the mathematical model of the process that is considered unknown [1]–[8]

$$y^{(v)}(t) = F(t) + \alpha u(t), \tag{1}$$

where $y^{(v)}(t) \in R$ is the v^{th} order derivative of the controlled output $y(t)$, with $v \geq 1$ being selected by the system designer, $F(t) \in R$ is a term that is permanently updated since it encapsulates the uncertain components of the process along with possible disturbances, $\alpha \in R$ is a constant parameter selected by the system designer such that $\alpha u(t)$ and $y(t)$ are of the same magnitude, and $u(t) \in R$ is the control input. For the empirical sensitivity study proposed in this paper, the derivative order will take values from 1 to 5 to generate a first-, second-, third-, fourth-,

and fifth-order ultra-local model expressed in discrete-time domain using the Euler discretization method:

$$\begin{aligned}
y(k+1) &= y(k) + F(k) + \alpha u(k),\\
y(k+2) &= 2y(k+1) - y(k) + F(k) + \alpha u(k),\\
y(k+3) &= 3y(k+2) - 3y(k+1) + y(k) + F(k) + \alpha u(k),\\
y(k+4) &= 4y(k+3) - 6y(k+2) + 4y(k+1) - y(k) + F(k) + \alpha u(k),\\
y(k+5) &= 5y(k+4) - 10y(k+3) + 10y(k+2) - 5y(k+1) + y(k) + F(k)\\
&\quad + \alpha u(k),
\end{aligned} \tag{2}$$

where $F(k) \in R$, $u(k) \in R$ and $y(k) \in R$ are the discrete-time expressions of $F(t)$, $u(t)$ and $y(t)$. The control laws of the first-, second-, third-, fourth-, and fifth-order MFC algorithm with PI component are [1]–[8]:

$$\begin{aligned}
u(k) &= -[\hat{F}(k) - r(k+1) + r(k) + k_1 e(k) + k_2 e(k-1)]/\alpha,\\
u(k) &= -[\hat{F}(k) - r(k+2) + 2r(k+1) - r(k) + k_1 e(k) + k_2 e(k-1)]/\alpha,\\
u(k) &= -[\hat{F}(k) - r(k+3) + 3r(k+2) - 3r(k+1) + r(k) + k_1 e(k) + k_2 e(k-1)]/\alpha,\\
u(k) &= -[\hat{F}(k) - r(k+4) + 4r(k+3) - 6r(k+2) + 4r(k+1) - r(k) + k_1 e(k)\\
&\quad + k_2 e(k-1)]/\alpha,\\
u(k) &= -[\hat{F}(k) - r(k+5) + 5r(k+4) - 10r(k+3) + 10r(k+2) - 5r(k+1) + r(k)\\
&\quad + k_1 e(k) + k_2 e(k-1)]/\alpha,
\end{aligned} \tag{3}$$

where $k_1 \in R$ and $k_2 \in R$ are the proportional and integrator gains of the MFC algorithm, $\mathbf{K} = [k_1, k_2]^T$, $r(k) \in R$ is the output of the reference model, $\hat{F}(k) \in R$ is the estimate of $F(k) \in R$ and is generated online using the I/O data of the controlled process from first-, second-, third-, fourth-, and fifth-order ultra-local model in (2) [1]–[8]:

$$\begin{aligned}
\hat{F}(k) &= y(k+1) - y(k) - \alpha u(k),\\
\hat{F}(k) &= y(k+2) - 2y(k+1) + y(k) - \alpha u(k),\\
\hat{F}(k) &= y(k+3) - 3y(k+2) + 3y(k+1) - y(k) - \alpha u(k),\\
\hat{F}(k) &= y(k+4) - 4y(k+3) + 6y(k+2) - 4y(k+1) + y(k) - \alpha u(k),\\
\hat{F}(k) &= y(k+5) - 5y(k+4) + 10y(k+3) - 10y(k+2) + 5y(k+1) - y(k)\\
&\quad - \alpha u(k).
\end{aligned} \tag{4}$$

Since $\hat{F}(k)$ estimates $F(k)$, the difference between these two terms is the estimation error

$$\delta(k) = F(k) - \hat{F}(k) \approx 0, \tag{5}$$

and it is regarded as a negligible disturbance in the design of the first-, second-, third-, fourth-, and fifth-order MFC algorithms.

The steps used in the design of the discrete-time first-, second-, third-, fourth-, and fifth-order MFC algorithm are:

Step 1.1. Parameter $\alpha \in R$ should be set by the designer to ensure that $\alpha u(k)$ and $y(k+1)-y(k)$ are of the same magnitude in the first-order MFC algorithm, $\alpha u(k)$ and $y(k+2)-2y(k+1)+y(k)$ are of the same magnitude in the second-order MFC algorithm, $\alpha u(k)$ and $y(k+3)-3y(k+2)+3y(k+1)-y(k)$ are of the same magnitude in the third-order MFC algorithm, $\alpha u(k)$ and $y(k+4)-4y(k+3)+6y(k+2)-4y(k+1)+y(k)$ are of the same magnitude in the fourth-order MFC algorithm, and $\alpha u(k)$ and $y(k+5)-5y(k+4)+10y(k+3)-10y(k+2)+5y(k+1)-y(k)$ are of the same magnitude in the fifth-order MFC algorithm.

Step 1.2. Parameters $k_1 \in R$ and $k_2 \in R$ of $\mathbf{K}=[k_1,k_2]^T$ of the MFC algorithms should be set by the designer ensuring that the closed-loop control system delivers a proper performance index value.

2.2. The MFC-FRIT algorithms

In the mix between first-, second-, third-, fourth-, and fifth-order MFC algorithm with FRIT is proposed to determine the optimal value of $\mathbf{K}=[k_1,k_2]^T$ with the notation $\mathbf{K}^*=[k_1^*,k_2^*]^T$, which matches the PI gains of the MFC algorithm by solving the optimization problem via a trust region algorithm [14]–[16], [20]

$$\mathbf{K}^*=\arg\min_{\mathbf{K}} J_{FRIT}(\mathbf{K}),\ J_{FRIT}(\mathbf{K})=\frac{1}{N}\sum_{k=1}^{N}[y_0(\mathbf{K}^{(0)},k)-\tilde{y}_{\mathbf{K}}(\mathbf{K},k)]^2, \tag{6}$$

where N is the number of samples. In the MFC-FRIT mix, superscript 0 is used to highlight the data and parameters from the initial closed-loop experiment with MFC algorithms. Therefore $y_0(\mathbf{K}^{(0)},k)$ is the output generated after the initial experiment, and $\tilde{y}_{\mathbf{K}}(\mathbf{K},k)$ is the fictitious reference output that is determined offline using the fictitious reference input $\tilde{r}(\mathbf{K},k)$ (virtual set-point) and a reference model $\mathrm{M}(q^{-1})$:

$$\tilde{y}_{\mathbf{K}}(\mathbf{K},k)=\mathrm{M}(q^{-1})\tilde{r}(\mathbf{K},k). \tag{7}$$

The reference model $\mathrm{M}(q^{-1})$ is set by the designer and it is chosen to satisfy the performance requirements set for the control system. The fictitious reference input is computed using the sum of the initial output $y_0(\mathbf{K}^{(0)},k)$ and inverse controller and the initial control input $u_0(\mathbf{K}^{(0)},k)$ [14]–[16], [20]

$$\tilde{r}_{\mathbf{K}}(\mathbf{K},k)=C(\mathbf{K},q)^{-1}u_0(\mathbf{K}^{(0)},k)+y_0(\mathbf{K}^{(0)},k) \tag{8}$$

where $C(\mathbf{K},q)^{-1}$ is the inverse transfer function of the PI component of the MFC algorithms expressed as

$$C(\mathbf{K},q)^{-1}=k_1q+k_2q^{-1}. \tag{9}$$

The tuning process is made using the I/O data generated after an initial closed-loop experiment. Parameter α will remain chosen by the control system designer.

Since FRIT is an iterative algorithm, $\mathbf{K}$ is iteratively updated using a trust region algorithm:

$$\mathbf{K}^{(i+1)}=\mathbf{K}^{(i)}+\mathbf{p}^{(i)}, \tag{10}$$

where $\mathbf{p}^{(i)}$ is the search ratio direction [1], [36]:

$$\mathbf{p}^{(i)} = \frac{f(\mathbf{K}^{(i)} + \mathbf{p}^{(i)}) - f(\mathbf{K}^{(i)})}{\Phi^{(i)}(\mathbf{p}^{(i)}) - \Phi^{(i)}(\mathbf{0})}, \tag{11}$$

and is obtained as a solution to the quadratic problem:

$$\Phi^{(i)}(\mathbf{p}) = J^{(i)} + (\mathbf{g}^{(i)})^T\mathbf{p} + \frac{1}{2}\mathbf{p}^{(T)}\mathbf{G}^{(i)}\mathbf{p} \quad \text{s.t.: } \|\mathbf{p}\| \leq \Delta^{(i)}, \tag{12}$$

where $\Delta^{(i)} > 0$ is a given margin, which specifies the radius of the sphere centered at $\mathbf{K}^{(i)}$ (the sphere is the trust region), $\mathbf{g}^{(i)}$ the gradient of the objective function in (6), and $\mathbf{G}^{(i)}$ is an approximation of the Hessian of J [1], [36]. According to [20], the MFC-FRIT algorithm assumes that the data-pair $(u_0(\mathbf{K}^{(0)}, k), y_0(\mathbf{K}^{(0)}, k))$ are non-trivial, $\tilde{e}(\mathbf{K}, k) = (y_0(\mathbf{K}^{(0)}, k) - \tilde{y}_{\mathbf{K},k}(\mathbf{K}, k))$ is the fictitious error, and therefore [14]–[16], [20]:

$$\lim_{\mathbf{K}\to\mathbf{K}^*} \sum_{k=1}^{N} (y(\mathbf{K}, k) - \tilde{y}(\mathbf{K}, k))^2 = \lim_{\mathbf{K}\to\mathbf{K}^*} \sum_{k=1}^{N} (e^2(\mathbf{K}, k)). \tag{13}$$

The block diagram of the control system of the MFC-FRIT algorithm is depicted in Fig. 1. This diagram is generally used in the first-, second-, third-, fourth-, and fifth-order MFC-FRIT algorithms.

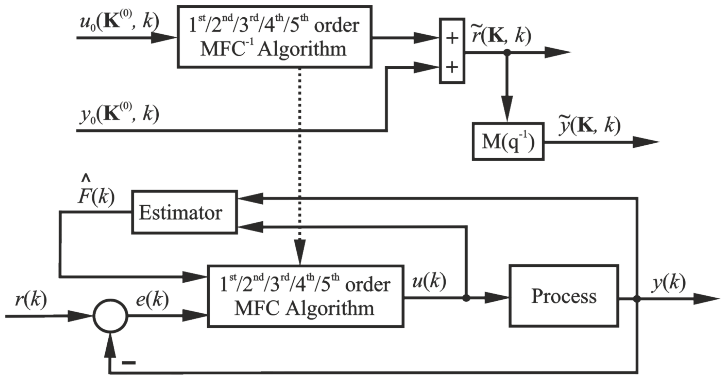

Fig. 1. The block diagram of the control system structure with the MFC-FRIT algorithm.

The steps used in the design of the discrete-time first-, second-, third-, fourth-, and fifth-order MFC-FRIT algorithms are:

Step 2.1. The control system designer should follow Step 1.1 of the discrete-time first-, second-, third-, fourth-, and fifth-order MFC algorithms. In this stage, the designer should set the value of $\alpha \in R$ to fulfill the conditions detailed in Step 1.1.

Step 2.2. The control system designer should follow Step 1.1 of the discrete-time first-, second-, third-, fourth-, and fifth-order MFC algorithms. In this step, the designer should set the value of $\mathbf{K} = [k_1, k_2]^T$ to fulfill the conditions detailed in Step 1.2. Use is made of $\mathbf{K} = \mathbf{K}^{(0)}$, which is the initial parameter vector of the MFC-FRIT algorithm.

Step 2.3. The initial real-time closed-loop experiment is performed, the fictitious reference input $\tilde{r}(\mathbf{K}, k)$ is offline computed in terms of (8) also using the collected I/O data pair $(u_0(\mathbf{K}^{(0)}, k), y_0(\mathbf{K}^{(0)}, k))$.

Step 2.4. The designer selects the reference model $\mathrm{M}(q^{-1})$ to ensure that its output meets the performance requirements imposed on the control system.

Step 2.5. The fictitious reference output $\tilde{y}_{\mathbf{K}}(\mathbf{K}, k)$ is computed offline in terms of (7).

Step 2.6. The optimal parameter vector $\mathbf{K}^*$ is determined by using the prior experiment's control error as the reference input in the gradient experiment to optimize the parameters of the PI component of the MFC algorithm in terms of (10) by means of a trust region algorithm.

Steps 2.3 through 2.6 are repeated several times to improve the overall control system performance. In Step 2.3, the data of the current experiment will be considered for a new iteration. In the current paper, five iterations are considered.

3. The 3D Crane Systems

The first-, second-, third-, fourth-, and fifth-order MFC and MFC-FRIT algorithms are validated using experiments on the 3D laboratory equipment to control the x-, y-, and z-axes. The nonlinear state-space mathematical model of the 3D crane is [19], [37]

$$
\begin{aligned}
\dot{x}_1 &= x_2,\\
\dot{x}_2 &= -T_1 x_2 - T_{sy}\operatorname{sgn}(x_2) - \mu_1\cos(x_5)[-T_3 x_{10} - T_{sz}\operatorname{sgn}(x_{10})] + k_1 u_1\\
&\quad + k_3\mu_1\cos(x_5)u_3,\\
\dot{x}_3 &= x_4,\\
\dot{x}_4 &= -T_2 x_4 - T_{sx}\operatorname{sgn}(x_4) - \mu_2\sin(x_5)\sin(x_7)[-T_3 x_{10} - T_{sz}\operatorname{sgn}(x_{10})]\\
&\quad + k_2 u_2 + k_3\mu_2\sin(x_5)\sin(x_7)u_3,\\
\dot{x}_5 &= x_6,\\
\dot{x}_6 &= -[T_1 x_2 - T_{sy}\operatorname{sgn}(x_2)]\sin(x_5)/x_9 + \sin(x_3)\cos(x_5)x_8^2/x_9\\
&\quad + \cos(x_5)\cos(x_7)[k_1\sin(x_5)u_1 - k_2\cos(x_5)\sin(x_7)u_2\\
&\quad - k_3\mu_2\sin(x_5)\cos(x_5)\sin^2(x_7)u_3 + k_3\mu_1\sin(x_5)\cos(x_5)u_3]/x_9^2\\
&\quad + \mu_2\sin(x_5)\cos(x_5)\sin^2(x_7)[-T_3 x_{10} - T_{sz}\operatorname{sgn}(x_{10})]/x_9\\
&\quad + \cos(x_5)\sin(x_7)[T_2 x_4 + T_{sx}\operatorname{sgn}(x_4)]/x_9 - \mu_1\sin(x_5)\cos(x_5)[-T_3 x_{10}\\
&\quad - T_{sz}\operatorname{sgn}(x_{10})]/x_9 - 2x_6 x_{10}/x_9,\\
\dot{x}_7 &= x_8,\\
\dot{x}_8 &= k_2\sin(x_7)\cos(x_7)u_2/[x_9^2\sin^2(x_5)] - k_3\mu_1\mu_2\sin^2(x_7)\cos(x_7)u_3/[x_9^2\sin(x_5)]\\
&\quad + \mu_2\sin(x_7)\cos(x_7)[-T_3 x_{10} - T_{sz}\operatorname{sgn}(x_{10})]/x_9 - 2x_8 x_{10}/x_9 + \cos(x_7)[T_2 x_4\\
&\quad + T_{sx}\operatorname{sgn}(x_4)]/[x_9\sin(x_5)],\\
\dot{x}_9 &= x_{10},\\
\dot{x}_{10} &= \cos(x_5)[T_1 x_2 + T_{sy}\operatorname{sgn}(x_2)] + x_8^2 x_9\sin^2(x_5) - k_1\sin(x_5)\cos(x_5)\cos(x_7)u_1\\
&\quad - k_2\sin^2(x_5)\sin(x_7)\cos(x_7)u_2 + k_3\sin(x_5)\cos(x_7)[-\mu_2\sin^2(x_5)\sin^2(x_7)\\
&\quad - \mu_1\cos^2(x_5) - 1]u_3 + \mu_2\sin^2(x_5)\sin^2(x_7)[-T_3 x_{10} - T_{sz}\operatorname{sgn}(x_{10})]\\
&\quad + \sin(x_5)\sin(x_7)[T_2 x_4 + T_{sx}\operatorname{sgn}(x_4)] + \mu_1[-T_3 x_{10} - T_{sz}\operatorname{sgn}(x_{10})]\\
&\quad + \mu_1\sin^2(x_5)[-T_3 x_{10} - T_{sz}\operatorname{sgn}(x_{10})] + x_6^2 x_9 - T_3 x_{10} - T_{sz}\operatorname{sgn}(x_{10}).
\end{aligned}
\tag{14}
$$

where $u_1 \in [-1,1]$, $u_2 \in [-1,1]$, $u_3 \in [-1,1]$ are the control inputs of the Pulse Width Modulation (PWM) duty cycles controlling the Direct Current (DC) motors, that actuate the 3D crane along the x-, y-, and z-axes, referred to as x_1, x_3 and x_9, respectively.

The significance of the state variables is: $x_1(m) = y_1(m)$ the cart's distance from the rail's center, x_2 the cart's speed in the x_1 direction, $x_3(m) = y_2(m)$ the distance of the rail and cart from the center of the construction frame, x_4 the cart's speed in the x_3, direction, x_5 the acute angle between the payload's lift-line and the rail, x_6 the angular speed corresponding to the x_5 direction, x_7 the acute angle formed between the payload's lift-line and the vertical axis, x_8 the angular speed corresponding to the x_7 direction, $x_9(m) = y_3(m)$ the lift-line length also known as payload's position, x_{10} the list's line speed.

4. Experiments and Results

The proposed first-, second-, third-, fourth-, and fifth-order MFC and MFC-FRIT algorithms are evaluated through several real-time experiments on the 3D crane system by controlling the x-, y-, and z-axes. The purpose of the MFC-FRIT algorithm is to reduce the tuning effort since the parameters of the MFC algorithms are optimally tuned by solving a gradient problem via a trust region algorithm. The purpose of the empirical sensitivity study of the first-, second-, third-, fourth-, and fifth-order MFC and MFC-FRIT algorithms is to determine whether there is a direct proportionality between controller complexity and improvements of the system performance, whether the algorithm order increases the captured dynamic behavior are crucial in improving the system's performances. The case study will also determine the proper order to be selected in designing the MFC-FRIT algorithms for the 3D crane systems. The performance improvements of the MFC versus MFC-FRIT algorithm are measured via the overall performance index

$$J_{e,u}(\mathbf{K}_{\diamondsuit}) = \sum_{k=1}^{N} \left[e_1^2(\mathbf{K}_{\diamondsuit 1}, k) + e_2^2(\mathbf{K}_{\diamondsuit 2}, k) + e_3^2(\mathbf{K}_{\diamondsuit 3}, k) \right], \tag{15}$$

where subscripts 1, 2, and 3 indicate the x-, y-, and z-axes, $\mathbf{K}_{\diamondsuit} = \begin{bmatrix} \mathbf{K}_{\diamondsuit 1} & \mathbf{K}_{\diamondsuit 2} & \mathbf{K}_{\diamondsuit 3} \end{bmatrix}$ while $\diamondsuit = \{\text{MFCi, MFCi-FRIT}\}$ representing the algorithm used with $i = 1, ..., 5$ represents the order of the MFC algorithm. The rest of the parameters have the same significance as in Section 2. The optimal parameters of the MFC-FRIT algorithms are determined via the optimization problem in (6) by computing the solution in terms of (10). The reference trajectory used in the control loop with the first-, second-, third-, fourth-, and fifth-order MFC and MFC-FRIT algorithms is

$$r_i(k) = y_i^*(k) H_{y_i^*(k)}(z), i \in \{1, 2, 3\}, \tag{16}$$

where:

$$H_{y_1^*(k)}(z) = \frac{0.04877}{z - 0.9512}, H_{y_2^*(k)}(z) = \frac{0.0465}{z - 0.9535}, H_{y_3^*(k)}(z) = \frac{0.03278}{z - 0.9672}, \tag{17}$$

$$
\begin{aligned}
&y_1^*(k) = 0.15 \text{ if } k \in [0, 20/T_s], 0.1 \text{ if } k \in (20/T_s, 35/T_s], -0.05 \text{ if } k \in (35/T_s, 50/T_s], \\
&\quad 0 \text{ if } k \in (50/T_s, 70/T_s], \\
&y_2^*(k) = 0 \text{ if } k \in [0, 5/T_s], 0.15 \text{ if } k \in (5/T_s, 25/T_s], -0.15 \text{ if } k \in (25/T_s, 40/T_s], \\
&\quad 0 \text{ if } k \in (40/T_s, 70/T_s], \\
&y_3^*(k) = 0 \text{ if } k \in [0, 15/T_s], 0.1 \text{ if } k \in (15/T_s, 30/T_s], -0.05 \text{ if } k \in (30/T_s, 45/T_s], \\
&\quad 0 \text{ if } k \in (45/T_s, 70/T_s].
\end{aligned} \tag{18}
$$

The control systems are characterized by a dynamic regime with the reference trajectory described in (16) through (18), a sampling time of $T_s = 0.01$ s a time range of 70 s, zero initial conditions, and no additive disturbances.

The design of the first-, second-, third-, fourth-, and fifth-order MFC algorithms is based on the steps in Subsection 2.1, i.e. parameter $\alpha = 0.005$ is set for the x-, y-, and z-axes by the designer to ensure that the conditions in Step 1.1 are fulfilled. Next, parameters

$$
\begin{aligned}
\mathbf{K}_{\text{MFC1}} &= [-0.1475\ -0.7446\ -8.2154\ -5.1011\ -0.9558\ -0.0716]^T, \\
\mathbf{K}_{\text{MFC2}} &= [-1.8015\ -1.0602\ -2.1285\ -1.1832\ -1.9971\ -0.3245]^T, \\
\mathbf{K}_{\text{MFC3}} &= [-1.7235\ -0.9541\ -1.8911\ -0.5248\ -2.4514\ -0.4561]^T, \\
\mathbf{K}_{\text{MFC4}} &= [-0.8024\ -0.6345\ -1.5415\ -0.1149\ -0.9891\ -0.7871]^T, \\
\mathbf{K}_{\text{MFC5}} &= [-1.9812\ -0.9951\ -12.7539\ -0.7546\ -2.9645\ -1.9542]^T,
\end{aligned} \tag{19}
$$

for the first-, second-, third-, fourth-, and fifth-order MFC algorithms, are set by the designer according to Step 2.1 to ensure that the closed-loop control system delivers a proper value of the performance index in (15).

The design implementation of the first-, second-, third-, fourth-, and fifth-order MFC-FRIT algorithms is performed using the step in Subsection 2.2, which means the parameter $\alpha = 0.005$ is set for the x-, y-, and z-axes by the designer to ensure that the conditions in Step 2.1 are fulfilled. Parameters $\mathbf{K}_\diamond$ are set to fulfill the conditions in Step 2.2 for the first-, second-, third-, fourth-, and fifth-order MFC-FRIT algorithms, in this case $\mathbf{K}_\diamond = \mathbf{K}_\diamond^{(0)}$ and the values of $\mathbf{K}_\diamond$ in (19) are the initial parameter vector of the MFC-FRIT algorithm. After performing the initial real-time closed-loop experiment, the I/O data pair is collected to compute offline the fictitious reference input $\tilde{r}(\mathbf{K}, k)$ in terms of (8) according to Step 2.3. The reference model $\mathrm{M}_i(z) = H_{y_i^*(k)}(z)$ is set by the designer by having the same transfer functions as in (17) to ensure that its output meets the performance requirements imposed on the control system according to Step 2.4. Next, the fictitious reference output $\tilde{y}_{\mathbf{K}}(\mathbf{K}, k)$ is determined offline in terms of (7) according to Step 2.5. Finally, the optimal parameter vector $\mathbf{K}_\diamond^*$

$$
\begin{aligned}
\mathbf{K}_{\text{MFC1-FRIT}} &= [-0.1311\ -0.7121\ -8.1813\ -5.2178\ -0.9947\ -0.0598]^T, \\
\mathbf{K}_{\text{MFC2-FRIT}} &= [-1.9124\ -0.6612\ -2.0271\ -1.1781\ -1.8124\ -0.2984]^T, \\
\mathbf{K}_{\text{MFC3-FRIT}} &= [-1.7155\ -0.8713\ -1.8512\ -0.5184\ -2.5001\ -0.3124]^T, \\
\mathbf{K}_{\text{MFC4-FRIT}} &= [-0.8123\ -0.7344\ -1.6116\ -0.1103\ -1.1983\ -0.9072]^T, \\
\mathbf{K}_{\text{MFC5-FRIT}} &= [-1.9811\ -0.8962\ -12.1311\ -0.6646\ -2.8954\ -1.8154]^T,
\end{aligned} \tag{20}
$$

of the first-, second-, third-, fourth-, and fifth-order MFC algorithms are computed after five iterations by solving the optimization problem (6) using a trust region algorithm in terms of (10).

The experimental results obtained after following Steps 1.1 and 1.2 for the MFC algorithms and Steps 2.1 through 2.6 for the MFC-FRIT algorithms are presented in a summarized manner Table 1, and also separately in Figs. 2 through 6 of the supplementary material [38] associated to this paper. The results are obtained by averaging ten sets of experiments for each control system structure to eliminate the random disturbances that can appear during real-time experiments.

Table 1. The average and the variance of the performance index $J_{e,u}$ index for the MFC and MFC-FRIT algorithms

Algorithm	Average of $J_{e,u}$	Variance of $J_{e,u}$
1st order MFC	$3.2393 \cdot 10^{-4}$	$1.5023 \cdot 10^{-12}$
1st order MFC-FRIT	$2.3379 \cdot 10^{-4}$	$4.0095 \cdot 10^{-13}$
2nd order MFC	$3.1683 \cdot 10^{-4}$	$7.9362 \cdot 10^{-13}$
2nd order MFC-FRIT	$2.3176 \cdot 10^{-4}$	$2.2211 \cdot 10^{-13}$
3rd order MFC	$3.0536 \cdot 10^{-4}$	$7.0035 \cdot 10^{-13}$
3rd order MFC-FRIT	$2.2520 \cdot 10^{-4}$	$1.4721 \cdot 10^{-13}$
4th order MFC	$2.9991 \cdot 10^{-4}$	$8.4988 \cdot 10^{-13}$
4th order MFC-FRIT	$2.1876 \cdot 10^{-4}$	$2.0935 \cdot 10^{-13}$
5th order MFC	$2.6991 \cdot 10^{-4}$	$7.7573 \cdot 10^{-13}$
5th order MFC-FRIT	$1.9859 \cdot 10^{-4}$	$2.9637 \cdot 10^{-13}$

The reference trajectory and output responses illustrated in [38] show that the performance of the MFC algorithms is improved by mixing them with FRIT. Even if a higher-order MFC algorithm should precisely approximate the system behavior due to system dynamics, the performances between the first-, second-, third-, fourth-, and fifth-order MFC are good, but not satisfying since a higher-order MFC is more complex in implementation and design. According to the data in Table 1, the average of $J_{e,u}$ in the case of the MFC algorithms is that $J_{e,u\,\text{MFC5}} \approx 0.90 \cdot J_{e,u\,\text{MFC4}}$, $J_{e,u\,\text{MFC4}} \approx 0.98 \cdot J_{e,u\,\text{MFC3}}$, $J_{e,u\,\text{MFC3}} \approx 0.96 \cdot J_{e,u\,\text{MFC2}}$, $J_{e,u\,\text{MFC2}} \approx 0.98 \cdot J_{e,u\,\text{MFC1}}$. Performing a similar comparison in the case of the MFC-FRIT algorithms is that $J_{e,u\,\text{MFC5-FRIT}} \approx 0.91 \cdot J_{e,u\,\text{MFC4-FRIT}}$, $J_{e,u\,\text{MFC4-FRIT}} \approx 0.97 \cdot J_{e,u\,\text{MFC3-FRIT}}$, $J_{e,u\,\text{MFC3-FRIT}} \approx 0.97 \cdot J_{e,u\,\text{MFC2-FRIT}}$, $J_{e,u\,\text{MFC2-FRIT}} \approx 0.73 \cdot J_{e,u\,\text{MFC1-FRIT}}$. There is no doubt that a higher-order MFC performs better than a less-order MFC algorithm, therefore there is a direct proportionality between controller complexity and improvements in the system performance. Therefore, the authors' recommendation for 3D crane processes is to use a first-order MFC algorithm due to its efficiency and simplicity.

The improvements after five iterations by using the FRIT are clear and using the data in Table 1 of the average of $J_{e,u}$ results in the following ratios between the MFC-FRIT and the MFC algorithms, i.e. $J_{e,u\,\text{MFC1-FRIT}} \approx 0.72 \cdot J_{e,u\,\text{MFC1}}$, $J_{e,u\,\text{MFC2-FRIT}} \approx 0.73 \cdot J_{e,u\,\text{MFC2}}$, $J_{e,u\,\text{MFC3-FRIT}} \approx 0.74 \cdot J_{e,u\,\text{MFC3}}$, $J_{e,u\,\text{MFC4-FRIT}} \approx 0.73 \cdot J_{e,u\,\text{MFC4}}$, $J_{e,u\,\text{MFC5-FRIT}} \approx 0.74 \cdot J_{e,u\,\text{MFC5}}$.

5. Conclusions

The current paper successfully proposed the mix between the MFC and FRIT algorithms since they have complementary features. The higher-order MFC and the MFC-FRIT algorithms were validated using experiments on 3D crane laboratory equipment. The optimal parameters of MFC algorithms were computed iteratively using FRIT after solving a gradient problem via a trust region algorithm. Therefore, the MFC-FRIT algorithms reduce the tuning effort since the MFC parameters are optimally tuned. The current work also showed how a higher-order MFC improves the performance of the control loop, and the best choice for 3D crane systems.

Future work will be related to validating the proposed MFC-FRIT algorithm on other types of processes, improving data-driven algorithms, and validating them on different types of processes. Such processes and control algorithms include piezoelectric active laminated shells [39], heart rate variability [40], navigation fuzzy cognitive maps [41], ad-hoc networks [42], bin packing [43], cascade control focusing on maglev trains [44] and telesurgical applications [45], two-mass systems [46], emergency facilities [47], robust evolving cloud control [48], fixed-time control [49], fuzzy control [50]–[52], and data-driven control [53].

Acknowledgements. This work was supported by a grant of the Romanian Ministry of Research, Innovation and Digitization, CNCS/CCCDI - UEFISCDI, project number ERANET-ENUAC-e-MATS, and by the NSERC of Canada.

References

[1] R.-E. PRECUP, R.-C. ROMAN and A. SAFAEI, *Data-Driven Model-Free Controllers* (1st edition), CRC Press, Taylor & Francis, Boca Raton, FL, 2021.

[2] M. FLIESS and C. JOIN, *Model-free control*, International Journal of Control, **86**(12), 2013, pp. 2228–2252.

[3] M. FLIESS and C. JOIN, *An alternative to proportional-integral and proportional-integral-derivative regulators: Intelligent proportional-derivative regulators*, International Journal of Robust and Nonlinear Control **32**(18), 2012, pp. 9512–9524.

[4] M. FLIESS, C. JOIN and D. SAUTER, *Defense against DoS and load altering attacks via model-free control: A proposal for a new cybersecurity setting*, Proceedings of 2021 5th International Conference on Control and Fault-Tolerant Systems, Saint-Raphael, France, 2021, pp. 58–65.

[5] C. JOIN, D. B. JOVELLAR, E. DELALEAU and M. FLIESS, *Detection and suppression of epileptiform seizures via model-free control and derivatives in a noisy environment*, Proceedings of IEEE 12th International Conference on Systems and Control, Batna, Algeria, 2024, pp. 1–6.

[6] M. MORENO-GONZALEZ, A. ARTUEDO, J. VILLAGRA, C. JOIN and M. FLIESS, *Speed-adaptive model-free lateral control for automated cars*, IFAC-PapersOnLine **55**(34), 2022, pp. 84–89.

[7] Q. GUILLOTEAU, B. ROBU, C. JOIN, M. FLIESS, E. RUTTEN and O. RICHARD, *Model-free control for resource harvesting in computing grids*, Proceedings of 2022 6th IEEE Conference on Control Technology and Applications, Trieste, Italy, 2022, pp. 1–7.

[8] D. HE, H. WANG, Y. TIAN and M. FLIESS, *MIMO ultra-local model-based adaptive enhanced model-free control using extremum-seeking for coupled mechatronic systems*, ISA Transactions **157**, 2025, pp. 233–247.

[9] P.-A. GEDOUIN, E. DELALEAU, J.-M. BOURGEOT, C. JOIN, S. A. CHIRANI and S. CALLOCH, *Experimental comparison of classical PID and model-free control: Position control of a shape memory alloy active spring*, Control Engineering Practice **19**(5), 2011, pp. 433–441.

[10] R.-C. ROMAN, R.-E. PRECUP, S. PREITL, C.-A. BOJAN-DRAGOS, A.-I. SZEDLAK-STINEAN and E.-L. HEDREA, *Data-driven control algorithms for shape memory alloys*, Proceedings of 2022 IEEE Conference on Control Technology and Applications, Trieste, Italy, 2022, pp. 1306–1312.

[11] D. WALEED and L. A. DUFFAUT ESPINOSA, *Simultaneous parameter estimation in model-free control*, Proceedings of 2024 American Control Conference, Toronto, ON, Canada, 2024, pp. 480–485.

[12] X. ZOU, Z. LIU, B. WANG, W. ZHAO and Q. DANG, *Model-free control-based trajectory tracking control of a tail-sitter UAV in hovering mode*, IEEE Transactions on Instrumentation and Measurement **73**, 2024, paper 3517820.

[13] P. M. SCHERER, A. OTHMANE and J. RUDOLPH, *Model-free control of a magnetically supported plate*, Control Engineering Practice **148**, 2024, paper 105950.

[14] R.-C. ROMAN, R.-E. PRECUP, E. M. PETRIU, M. MUNTYAN and E.-L. HEDREA, *Fictitious reference iterative tuning of intelligent proportional-integral controllers for tower crane systems*, Proceedings of 2023 31st, Mediterranean Conference on Control and Automation, Limassol, Cyprus, 2023, pp. 740–746.

[15] R.-C. ROMAN, R.-E. PRECUP and E.-L. HEDREA, *Intelligent proportional controller tuned by virtual reference feedback tuning and fictitious reference iterative tuning*, Procedia Computer Science **221**, 2023, pp. 86–93.

[16] R.-C. ROMAN, R.-E. PRECUP, E. M. PETRIU and M. MUNTYAN, *Fictitious reference iterative tuning of discrete-time model-free control for tower crane systems*, Studies in Informatics and Control **32**(1), 2023, pp. 5–14.

[17] R.-C. ROMAN, R.-E. PRECUP and R.-C. DAVID, *Second order intelligent proportional-integral fuzzy control of twin rotor aerodynamic systems*, Procedia Computer Science, **139**, 2018, pp. 372–380.

[18] R.-E. PRECUP, R.-C. ROMAN, T.-A. TEBAN, A. ALBU, E. M. PETRIU and C. POZNA, *Model-free control of finger dynamics in prosthetic hand myoelectric-based control systems*, Studies in Informatics and Control **29**(4), 2020, pp. 399–410.

[19] R.-E. PRECUP, R.-C. ROMAN, E.-L. HEDREA, E. M. PETRIU and C.-A. BOJAN-DRAGOS, *Data-driven model-free sliding mode and fuzzy control with experimental validation*, International Journal of Computers Communications & Control **16**(1), 2021, pp. 1–17.

[20] S. SOMA, O. KANEKO and T. FUJII, *A new method of controller parameter tuning based on input-output data – Fictitious Reference Iterative Tuning (FRIT)*, IFAC Proceedings Volumes, **37**(12), 2004, pp. 789–794.

[21] O. KANEKO, S. SOMA and T. FUJII, *A Fictitious Reference Iterative Tuning (FRIT) in the two-degree of freedom control scheme and its application to closed loop system identification*, IFAC Proceedings Volumes **38**(1), 2005, pp. 626–631.

[22] O. KANEKO, *Data-driven controller tuning: FRIT approach*, IFAC Proceedings Volumes **46**(11), 2013, pp. 326–336.

[23] H. IKEDA, K. GOTO, F. ZHANG, K. KAYASHIMA and T. HANAMOTO,*Application of fictitious reference iterative tuning to controller design for various machines*, Proceedings of 2018 International Power Electronics Conference, Niigata, Japan, 2018, pp. 1315–1321.

[24] A. YONEZAWA, H. YONEZAWA, D. YAHAGI and I. KAJIWARA, *Practical one-shot data-driven design of fractional-order PID controller: Fictitious reference signal approach*, ISA Transactions **152**, 2024, pp. 208–216.

[25] M. SEKINE, S. TSURUHARA and K. ITO, *MPC for artificial muscles using FRIT based optimized pseudo linearization model*, IFAC-PapersOnLine **56**(2), 2023, pp. 7264–7269.

[26] M. SEKINE, S. TSURUHARA and K. ITO, *Optimized design of a pseudo-linearization-based model predictive controller: Direct data-driven approach*, IET Control Theory & Applications, **19**(1), 2025, pp. 1–17.

[27] Z. K. K. LATT, H. SI and KANEKO, *Controller parameter tuning of a hexacopter with fictitious reference iterative tuning*, Proceedings of 2019 SICE International Symposium on Control Systems, Kumamoto, Japan, 2019, pp. 96–101.

[28] Z. LI, K. HIRAOKA and T. YAMAMOTO, *Design and experimental evaluation of a data-driven PID controller using cerebellar memory*, IET Control Theory & Applications **18**(11), 2024, pp. 1371–1382.

[29] Z. GAO, *Active disturbance rejection control: a paradigm shift in feedback control system design*, Proceedings of 2006 American Control Conference, Minneapolis, MN, USA, 2006, pp. 2399–2405.

[30] R.-C. ROMAN, R.-E. PRECUP, E. M. PETRIU and A.-I. BORLEA, *Hybrid data-driven active disturbance rejection sliding mode control with tower crane systems validation*, Romanian Journal of Information Science and Technology **27**(1), 2024, pp. 50–64.

[31] R.-C. ROMAN, R.-E. PRECUP and E. M. PETRIU, *Hybrid data-driven fuzzy active disturbance rejection control for tower crane systems*, European Journal of Control **58**, 2021, pp. 373–387.

[32] X.-N. HE and Z.-S. HOU, *Bipartite containment tracking for nonlinear MASs under FDI attack based on model-free adaptive iterative learning control*, Neurocomputing **614**, 2025, paper 128783.

[33] J. HUUSOM, H. HJALMARSSON, N. K. POULSEN and S. B. JØRGENSEN, *A design algorithm using external perturbation to improve iterative feedback tuning convergence*, Automatica **47**(12), 2011, pp. 2665–2670.

[34] S. FORMIENTIN, M. C. CAMPI, A. CARE and S. M. SAVARESI, *Deterministic continuous-time Virtual Reference Feedback Tuning (VRFT) with application to PID design*, Systems & Control Letters, **127**, 2019 pp. 25–34.

[35] R.-E. PRECUP, R.-C. ROMAN, E.-L. HEDREA and A.-I. SZEDLAK-STINEAN, *Classical and Modern Optimization Techniques Applied to Control and Modeling (1st edition)*, CRC Press, Taylor & Francis, Boca Raton, FL, Abingdon, 2025.

[36] L. GRIPPO and M. SCIANDRONE, *Introduction to Methods for Nonlinear Optimization*, Springer, Cham, UNITEXT, **152**, 2023.

[37] Inteco Ltd, *3D Crane, User's Manual*, Inteco, Krakow, 2012.

[38] R.-C. ROMAN, R.-E. PRECUP and E. M. PETRIU, Supplementary material of the paper Raul-Cristian ROMAN, Radu-Emil PRECUP, Emil M. PETRIU, *Higher-order model-free control tuned by fictitious reference iterative tuning for 3D cranes*, Romanian Journal of Information Science and Technology, 2025. Accessed: Mar. 3, 2025. [Online]. Available: https://uptro29158-my.sharepoint.com/:b:/g/personal/raul-cristian_roman_upt_ro/Ec6FTl4RIGdEmr9L6jl7Be0B6CsdNgspdeBA9i10u9pf3A?e=nDMkCg.

[39] P. MILIĆ, D. MARINKOVIĆ, S. KLINGE and Z. ĆOJBAŠIĆ, *Reissner-Mindlin based isogeometric finite element formulation for piezoelectric active laminated shells*, Tehnički Vjesnik **20**(2), 2023, pp. 416–425.

[40] C. ROTARIU, A. PASARICA, H. COSTIN and D. NEMESCU, *Spectral analysis of fetal heart rate variability associated with fetal acidosis and base deficit values*, Proceedings of 12th IEEE International Conference on Development and Application Systems, Suceava, Romania, 2014, pp. 210–213.

[41] J. VAŠČÁK, I. ZOLOTOVÁ and E. KAJÁTI, *Navigation fuzzy cognitive maps adjusted by PSO*, Proceedings of 23rd International Conference on System Theory, Control and Computing, Sinaia, Romania, 2019, pp. 107–112.

[42] S. I. BOUCETTA and Z. C. JOHANYÁK, *Optimized ad-hoc multi-hop broadcast protocol for emergency message dissemination in vehicular ad-hoc networks*, Acta Polytechnica Hungarica **19**(5), 2022, pp. 23–42.

[43] S. V. ROMERO, E. OSABA, E. VILLAR-RODRIGUEZ and A. ASLA, *Solving logistic-oriented bin packing problems through a hybrid quantum-classical approach*, Proceedings of 2023 IEEE 26th International Conference on Intelligent Transportation Systems, Bilbao, Spain, 2023, pp. 2239–2245.

[44] J. WEN and F.-L. WANG, *Stable levitation of single-point levitation systems for maglev trains by improved cascade control*, Romanian Journal of Information Science and Technology **27**(3–4), 2024, pp. 348–361.

[45] R.-E. PRECUP, T. HAIDEGGER, S. PREITL, B. BENYÓ, A. S. PAUL and L. KOVÁCS, *Fuzzy control solution for telesurgical applications*, Applied and Computational Mathematics **11**(3), 2012, pp. 378–397.

[46] P. KORONDI, H. HASHIMOTO and V. UTKIN, *Discrete sliding mode control of two mass system*, Proceedings of 1995 IEEE International Symposium on Industrial Electronics, Athens, Greece, 1995, pp. 338–343.

[47] Y.-Y. WANG, Z.-S. XU and F. G. FILIP, *A multi-objective model for the location of the emergency facilities and the selection of the rescue path based on the restoration of the damaged edges*, Studies in Informatics and Control **31**(3), 2022, pp. 5–20.

[48] I. ŠKRJANC, S. BLAŽIČ and P. ANGELOV, *Robust evolving cloud-based PID control adjusted by gradient learning method*, Proceedings of 2014 IEEE Conference on Evolving and Adaptive Intelligent Systems, Linz, Austria, 2014, pp. 1–6, 2014.

[49] Z.-B. LIN, J.-H. LIU, C. L. P. CHEN, G.-Y. LAI, Z.-Z. WU and Z. LIU, *Distributed fuzzy inverse optimal fixed-time control for uncertain multi-agent systems*, Information Sciences **652**, 2024, paper 119670.

[50] R.-E. PRECUP and S. PREITL, *Popov-type stability analysis method for fuzzy control systems*, Proceedings of Fifth European Congress on Intelligent Technologies and Soft Computing, Aachen, Germany, 1997, **3**, pp. 1306–1310.

[51] R.-E. PRECUP, S. PREITL, M. BĂLAŞ and V. BĂLAŞ, *Fuzzy controllers for tire slip control in anti-lock braking systems*, Proceedings of 2004 IEEE International Conference on Fuzzy Systems, Budapest, Hungary, 2004, **3**, pp. 1317–1322.

[52] H.-Y. ZHOU, H.-K. LAM, B. XIAO and C.-B. XUAN, *Integrated fault-tolerant control design with sampled-output measurements for interval type-2 Takagi-Sugeno fuzzy systems*, IEEE Transactions on Cybernetics **54**(9), 2024, pp. 5068–5077.

[53] Z.-X. MAO, M.-X. HOU and Z.-S. HOU, *Model-free adaptive bipartite consensus control for unknown heterogeneous nonlinear MASs with different input delays*, International Journal of Systems Science **55**(15), 2024, pp. 3114–3129.